Z. Phys. C - Particles and Fields 26, 191-198 (1984)

Zeitschrift für Physik C Particles and Fields

The Q^2 and Transverse Momentum Dependence of Jet Production in Photon-Photon Interactions

PLUTO Collaboration

Ch. Berger, A. Deuter, H. Genzel, W. Lackas, J. Pielorz[a], F. Raupach[b], and W. Wagner[c]
I. Physikalisches Institut der RWTH Aachen[d], D-5100 Aachen, Federal Republic of Germany

A. Klovning and E. Lillestöl
University of Bergen[e], N-5014 Bergen, Norway

J. Bürger[f], L. Criegee, F. Ferrarotto[g], G. Franke, M. Gaspero[g], Ch. Gerke[h], G. Knies, B. Lewendel, J. Meyer, U. Michelsen, K.H. Pape, B. Stella[g], U. Timm, G.G. Winter, M. Zachara[i], and W. Zimmermann
Deutsches Elektronen-Synchrotron (DESY), D-2000 Hamburg 52, Federal Republic of Germany

P.J. Bussey, S.L. Cartwright[j], J.B. Dainton, B.T. King, C. Raine, J.M. Scarr, I.O. Skillicorn, K.M. Smith, and J.C. Thomson
University of Glasgow[k], United Kingdom

O. Achterberg[l], V. Blobel, D. Burkart, K. Diehlmann, M. Feindt, H. Kapitza, B. Koppitz, M. Krüger[l], M. Poppe, H. Spitzer, and R. van Staa
II. Institut für Experimentalphysik der Universität Hamburg[d], D-2000 Hamburg 50, Federal Republic of Germany

Received 7 August 1984

C.Y. Chang, R.G. Glasser, R.G. Kellogg, S.J. Maxfield, R.O. Polvado[m], B. Sechi-Zorn, J.A. Skard, A. Skuja, A.J. Tylka, G.E. Welch, and G.T. Zorn
University of Maryland[n], USA

F. Almeida[o], A. Bäcker, F. Barreiro, S. Brandt, K. Derikum[p], C. Grupen, H.J. Meyer, H. Müller, B. Neumann, M. Rost, K. Stupperich, and G. Zech
Universität-Gesamthochschule Siegen[d], D-5900 Siegen, Federal Republic of Germany

G. Alexander, G. Bella, Y. Gnat, and J. Grunhaus
Tel-Aviv University[q], Tel-Aviv, Israel

H. Junge, K. Kraski, C. Maxeiner, H. Maxeiner, H. Meyer, D. Schmidt
Universität-Gesamthochschule Wuppertal[d], D-5600 Wuppertal, Federal Republic of Germany

Abstract. We present an experimental study of jet-production in photon-photon interactions for $0.1 \lesssim Q^2 \lesssim 120$ GeV^2 and jet transverse momentum, p_T, up to 5 GeV/c. At all Q^2, the data show a high p_T tail, characteristic of a point-like interaction. The jet production cross-section approaches the quark-parton model (QPM) expectation as either jet p_T or Q^2 increases. Overall, the data are well described in both total cross-section and event topology by the

[a] Deceased
[b] Now at University of Paris-Sud, F-91405 Orsay, France
[c] Now at University of California at Davis, California, USA
[d] Supported by the BMFT, Federal Republic of Germany
[e] Partially supported by Norwegian Council for Science and Humanities
[f] Currently on leave of absence at CERN, CH-1211 Geneva 23, Switzerland
[g] Rome University, partially supported by I.N.F.N., Sezione di Roma, Italy
[h] Now at CERN, CH-1211 Geneva 23, Switzerland
[i] Institute of Nuclear Physics, Ul. Kawiory 26a, PL-30055 Cracow, Poland
[j] Now at Rutherford Appleton Laboratory, Chilton, U.K.
[k] Supported by the U.K. Science and Engineering Research Council
[l] Now at Universität Karlsruhe, D-7500 Karlsruhe, Federal Republic of Germany
[m] Now at Northeastern University, Boston, Massachussetts, USA
[n] Partially supported by the Department of Energy, USA
[o] On leave of absence from Instituto de Fisica, Universidad Federal do Rio de Janeiro, Cidade Universitaria, 21910-Ilha do Fundao, RJ, Brasil
[p] Now at BESSY, D-1000 Berlin, Germany
[q] Partially supported by the Israeli Academy of Sciences and Humanities - Basic Research Foundation

sum of a vector-dominance model and a point-like interaction, represented by the QPM.

Introduction

It is generally accepted that hadron production in e^+e^- annihilation occurs primarily through creation of quark-antiquark pairs. In photon-photon ($\gamma\gamma$) interactions a similar mechanism is expected to contribute to hadron production due to the point-like component of the photon [1]. Hadron production would then take place through the reaction $\gamma\gamma \to q\bar{q}$ which can result in two jets of high transverse momentum (p_T) with respect to the $\gamma\gamma$-axis [2, 3]. This is in contrast to the familiar behaviour of the hadronic part of the photon which produces jets of particles of predominantly low transverse momentum relative to the $\gamma\gamma$-axis. Previous studies [4, 5] have shown evidence for the point-like part of the photon in jet production at large p_T in $\gamma\gamma$ interactions of nearly real photons. In this paper we report on an extended study of jet production by examining jets as a function of the squared mass of one of the virtual photons, $-Q^2$, as well as of p_T[6]. This enables us to study the evolution of the $\gamma\gamma$-interaction from what is expected to be a primarily hadronic interaction at low p_T and low Q^2 to a primarily point-like interaction at either high p_T or high Q^2. Such a study could also provide constraints on non-standard models of the strong interaction [7, 8].

The data presented here consist of events of the type

$$e^+e^- \to e^+e^- + \text{hadrons}$$

in the so-called "single-tag" mode in which only one of the scattered electrons is observed. The data were obtained using the PLUTO detector at the e^+e^- storage ring PETRA at an average e^+e^- center-of-mass energy of 34.7 GeV.

Apparatus

The details of the PLUTO detector have been given elsewhere [9]. Here we briefly discuss the components relevant to this study. Charged particles are detected and their momenta measured in the central detector, which consists of cylindrical proportional chambers in a 1.65 T solenoidal magnetic field, and two forward spectrometers, which are each composed of arrays of drift and proportional chambers and a 0.2 T-m septum magnet. The central detector covers the polar angular range $25° \lesssim \vartheta \lesssim 155°$ and the full azimuth. The forward spectrometers cover the regions $5° \lesssim \vartheta \lesssim 15°$ and $165° \lesssim \vartheta \lesssim 175°$, and 85% of the full azimuth. The momentum resolution of both the central detector and the forward spectrometers is $\sigma_p/p = 3\% \cdot p$ (p in GeV/c). Photons in the central region of the detector are measured in the barrel and endcap lead-scintillator shower counters, which cover 96% of the full solid angle.

The tagging electrons (as well as final-state photons) are measured in small-angle taggers (SAT's) and large angle taggers (LAT's) which cover the polar regions from 30 to 55 mrad and from 87 to 260 mrad, and in the endcaps which cover the range from 349 to 681 mrad. The SAT's are lead-scintillator shower counters with energy resolution $\sigma_E/E = 16.5\%/\sqrt{E}$, ($E$ in GeV). Each SAT is azimuthally segmented into twelve 30° modules, each of which is read out at the inner and outer radial edges using wavelength shifter bars. These signals, together with energy sharing between modules, provide a measurement of the shower position. Proportional tube chambers in front of the SAT's improve the position resolution and distinguish between charged particle and photon showers. This charge identification is important for reducing the background from e^+e^- annihilation with initial-state radiation. The LAT's are lead-scintillator shower counters with energy resolution $\sigma(E)/E = 25\%/\sqrt{E}$. Shower positions are determined by proportional tube chambers within the lead scintillator array. The LAT's are located immediately behind the forward spectrometers. By demanding that the LAT shower matches to a forward spectrometer track of appropriate charge and momentum, false tags due to photons or hadronic showers are suppressed. The endcaps are lead-scintillator counters interleaved by proportional chambers; they are segmented azimuthally into 12° sectors. The energy resolution is $\sigma(E)/E = 28\%/\sqrt{E}$. A detailed description of the endcap analysis is given in [10]. The Q^2 resolution over the angular range from 30 to 681 mrad is constant, $\sigma(Q^2)/Q^2 = 10\%$.

The experimental triggers for single-tagged events were made as loose as possible. For SAT-tagged events, the trigger required an SAT shower energy of at least 6 GeV in conjunction with at least one track in the central detector. This track trigger condition was fully efficient for tracks with $|\cos(\vartheta)| < 0.8$ and momentum transverse to the e^+e^- beam axis greater than 150 MeV/c. For LAT (endcap)-tagged events, a LAT (endcap) shower of more than 4 GeV (2.4 GeV), without any additional requirements, was sufficient to trigger the detector.

Data Selection and Background Estimates

In this study we consider only those events in which the tagging electron is measured with an energy greater than 8.0 GeV. To ensure that the photon emitted by the other electron is quasi-real we reject events with a SAT or LAT shower greater than 6.0 GeV on the opposite side of the detector from the tag. The mass distribution of the quasi-real photon (P^2) peaks at zero with 70% of the events having $P^2 < 0.01$ GeV^2.

Further restrictions were applied to the data to obtain a sample of well-reconstructed $\gamma\gamma$ events with minimal backgrounds. We required:

1. $|z_0| \leqq 35.0$ mm, where z_0 is the distance between the interaction vertex and the e^+e^- beam intersection point, as measured along the beam axis.

2. charged multiplicity $\geqq 4$.

3. $4.0 \leqq W_{\text{vis}} \leqq 13.0$ GeV, where W_{vis} is the visible invariant mass of the hadronic system, calculated from charged particles, assumed to be pions, and photons. Monte Carlo studies show that the mean ratio between the visible and the true invariant mass, W_{vis}/W, is approximately 0.75, with two thirds of the data between 0.5 and 1.0.

4. for endcap tagged events, the missing electron reconstructed using momentum conservation to have a momentum of at least 6 GeV along the beam axis opposite to the tag.

5. absolute of the charge of the hadronic system $\leqq 2$.

6. $|\sum \mathbf{p}_{Ti}| \leqq 3.0$ GeV/c, where $\mathbf{p}_{Ti}$ is the particle momentum transverse to the e^+e^- beams and the summation runs over all particles including the tag.

These selections reduce beam-gas events to a level less than 0.5%. The minimum multiplicity and W_{vis} requirements ensure that an analysis of the events in terms of jets is possible. The final two criteria suppress incomplete and badly measured events.

Other backgrounds are estimated using Monte Carlo techniques. We have considered backgrounds from the following reactions:

1. $e^+e^- \to$ hadrons.

2. $e^+e^- \to \tau^+\tau^-$.

3. $e^+e^- \to e^+e^-\tau^+\tau^-$.

4. $e^+e^- \to e^+e^-$ + hadrons, via the inelastic Compton process [1].

5. untagged $\gamma\gamma \to$ hadrons, in which a photon or showering hadron produces a false tag.

6. double-tagged $\gamma\gamma \to$ hadrons, in which one electron is erroneously treated as a hadron.

Table 1.

Tagger	$\int L \cdot dt$ (pb^{-1})	Q^2 range (GeV^2)	$\langle Q^2 \rangle$ (GeV^2)	Events
SAT	29.3	$0.1 \leqq Q^2 \leqq 1.0$	0.35	846
LAT	39.4	$1.0 \leqq Q^2 \leqq 18$	5.3	381
endcap	40.1	$15 \leqq Q^2 \leqq 120$	49	50

For the LAT and SAT tagged events backgrounds (1) and (3) are found to be important for high p_T jets. They give contaminations of (3.0 $\pm$0.2)% and (5.2 $\pm$ 0.5)% for SAT events and LAT events, respectively. At jet p_T greater than 2.0 GeV/c, these backgrounds are about 20% of the signal for the SAT events and 10% for the LAT events. These backgrounds are subtracted from all plots shown below. In the high Q^2 range (endcap tagged events) contamination of type (3) gives a background of (5 $\pm$3)%, while 7 events of type (1) are identified and eliminated by a visual inspection. Of the remaining backgrounds, (2) and (4) are negligible and the effect of (6) has been included in the Monte Carlo simulation. Background (5) is found to be unimportant for the LAT and endcap events but may contribute a few percent background for the SAT events at low jet p_T.

The number of events obtained with the above selections after background subtraction, the luminosities collected with the different trigger types, the corresponding Q^2 ranges and mean Q^2 values, are given in Table 1.

Models for Photon-Photon Interactions

The observed distributions of the parameters describing the interactions are influenced by the resolution and acceptance of the apparatus. To correct for this, either the measured quantities can be unfolded or the results can be compared with phenomenological models in which the influence of the apparatus is included; we here adopt the latter scheme. We consider two models which represent two basic processes of hadron production by a $\gamma\gamma$ interaction, namely the Quark Parton Model (QPM) and the Vector Dominance Model (VDM). The models are used to generate Monte Carlo events which are passed through a detector simulation and the data selections and analysis described above. We now briefly describe the models.

(1) QPM. The Vermaseren event generator [11] for $e^+e^- \to e^+e^-\mu\mu$ is used to produce fractionally charged quark pairs with masses of 300 MeV for u

and d, 500 MeV for s, and 1.6 GeV for c quarks. These quarks are then fragmented according to the Field-Feynmann prescription [12]. In particular, the light quarks are fragmented using $dN/dk_T^2 \sim \exp \cdot(-k_T^2/\sigma^2)$ with $\sigma = 350$ MeV/c, $f(z) = 1 - a + 3a(1-z)^2$ with $a = 0.77$, $P/(P+V) = 0.5$, and a sea quark ratio of $u:d:s = 2:2:1$; here the notation follows that used by Field and Feynmann [12]. For charm fragmentation we use the harder fragmentation function given in [13]. These parameters are standard, and are known to describe well $e^+e^- \to q\bar{q}$ at comparable hadronic center-of-mass energies [14].

We have studied the sensitivity of the QPM to variations in the light quark masses and fragmentation parameters. We find that a reduction of the quark mass to 10 MeV has negligible effect on the cross-section for jet production for $p_T \gtrsim 1.5$ GeV/c. Similarly, variation of the fragmentation parameters over wide ranges of values ($250 \leqq \sigma \leqq 500$ MeV/c, $0.30 \leqq a \leqq 0.9$, and $0.25 \leqq P/(P+V) \leqq 1.0$) leads to changes in the jet acceptance for $p_T \gtrsim 1.5$ GeV/c of 5–10%. Thus, within our kinematical range and statistics the comparison between the QPM and the observed number of high p_T events is insensitive to assumptions about quark masses and fragmentation.

(2) VDM. The second model is characterised by a specific Q^2 and W dependence of the cross section and a different set of fragmentation parameters. The fragmentation is again that of Field and Feynmann. The direction of the primary quarks is distributed so that the quark transverse momentum follows an $\exp(-5p_T^2)$ dependence with respect to the $\gamma\gamma$-axis. For the cross section we use a factorisation of the form $\sigma(W, Q^2) = \sigma(W) \cdot F(Q^2)$. The function $F(Q^2)$ we take from the Generalized Vector Dominance Model (GVDM) [15, 16]. The W-dependence $\sigma(W)$ at fixed Q^2 is assumed to be constant. To determine the cross section and the fragmentation parameters we adjust the free parameters of the model by comparison with SAT-tagged events in which the reconstructed jet axis is at small angles to the $\gamma\gamma$-axis. Our parametrization of the VDM cross section is $\sigma_{\gamma\gamma}(Q^2) = 240 \cdot F(Q^2)$ nb. The distributions of charged and neutral multiplicities, thrust, and particle momenta transverse to the reconstructed jet axis are well described by hadronization according to Field-Feynman fragmentation with non-standard values of $a = 0.45$ and $\sigma = 450$ MeV/c.

To study the systematic uncertainties of the VDM. we have varied the fragmentation parameters a and σ within the ranges 0.40–0.77 and 350–450 MeV, respectively. Also the jet axis has been rotated and tilted so that an intrinsic jet transverse momentum of the form $dN/dp_T^2 \propto \exp(-2p_T^2)$ (p_T in GeV/c) was introduced. These variations give rise to a band of VDM predictions shown in the figures below; they consequently imply a change in the normalizations of the VDM of $\pm 20\%$.

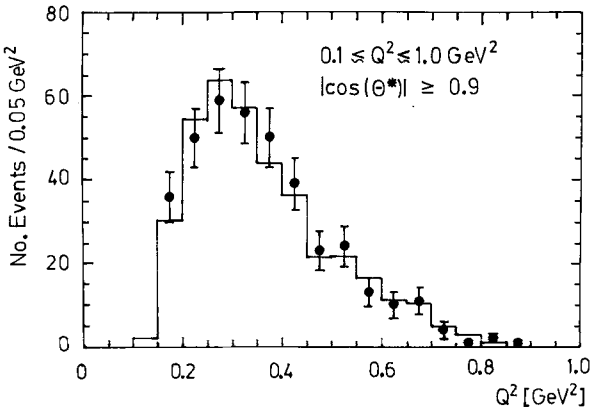

Fig. 1. Q^2 distribution for events with small jet angle with respect to the $\gamma\gamma$ direction. The solid curve is the prediction of VDM

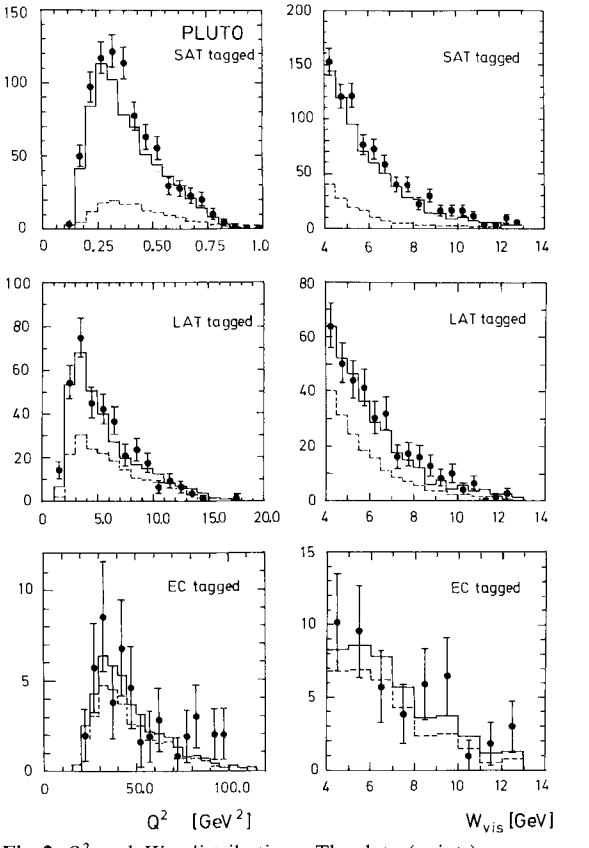

Fig. 2. Q^2 and W_{vis} distributions. The data (points) are compared with the sum of QPM and VDM (solid line). The dashed line shows the contribution from the QPM alone

In Fig. 1 we show the observed Q^2-distribution for SAT events where the angle, Θ^*, between the $\gamma\gamma$-axis and the reconstructed jet axis is small

($|\cos\Theta^*| \geqq 0.9$). In this region the data are expected to be dominated by VDM type events; we therefore compare this distribution with the VDM expectation. The good agreement between the model and our data justifies the GVDM ansatz. In Fig. 2a–f we give the Q^2 and W_{vis} distributions for the full Θ^* range and compare them with the QPM and VDM results. The W distribution is well described by a superposition of both models, although there is some evidence for excess events in the low Q^2 range around $Q^2 = 0.3\,\text{GeV}^2$. Overall the superposition of the two models gives a good description of the $Q^2 - W$ evolution of the data and leads us to use the models to study the topological characteristics of the events.

We emphasize that all distributions in this paper are uncorrected and hence can only be compared with other models after the influence of the PLUTO detector has been correctly simulated.

Jet Analysis of Data

For the further analysis of the data the $\gamma\gamma$ final state is transformed into its center of mass frame (CM). To search for jets in the events we make a thrust analysis. The transverse momentum, p_T, of the jet is defined with respect to the $\gamma\gamma$-axis as $p_T = |\mathbf{p}| \cdot \sin(\Theta^*)$, where $\mathbf{p}$ is the jet momentum along the thrust axis and Θ^* is the angle between the thrust axis and the $\gamma\gamma$-axis in the hadronic CM-frame. The $\gamma\gamma$-axis is determined from the incoming beams, the outgoing tagged electron or positron, and the observed boost of the hadronic system.

Results

Jets, regardless of the mechanism by which they are produced, are characterized by a limitation of k_T, the momentum of produced particles transverse to the thrust axis. This is in contrast to the longitudinal component of momentum, k_L, which grows almost linearily with W_{vis}. In Fig. 3a–f we plot $\langle k_T \rangle$ and $\langle k_L \rangle$ for charged hadrons as a function of W_{vis}, and compare the data with expectations from an all pion isotropic phase space model of hadronisation and a jet model, which is an incoherent sum of the QPM and the VDM models described above. Both the k_T limitation and the growth of k_L observed in the data are well described by the jet model. From the figure it is evident that particle momenta transverse to the thrust axis are limited, thus demonstrating the two-jet structure of the event topology. In addition, the clear difference between phase space and jet models also shows that experimental effects and the method

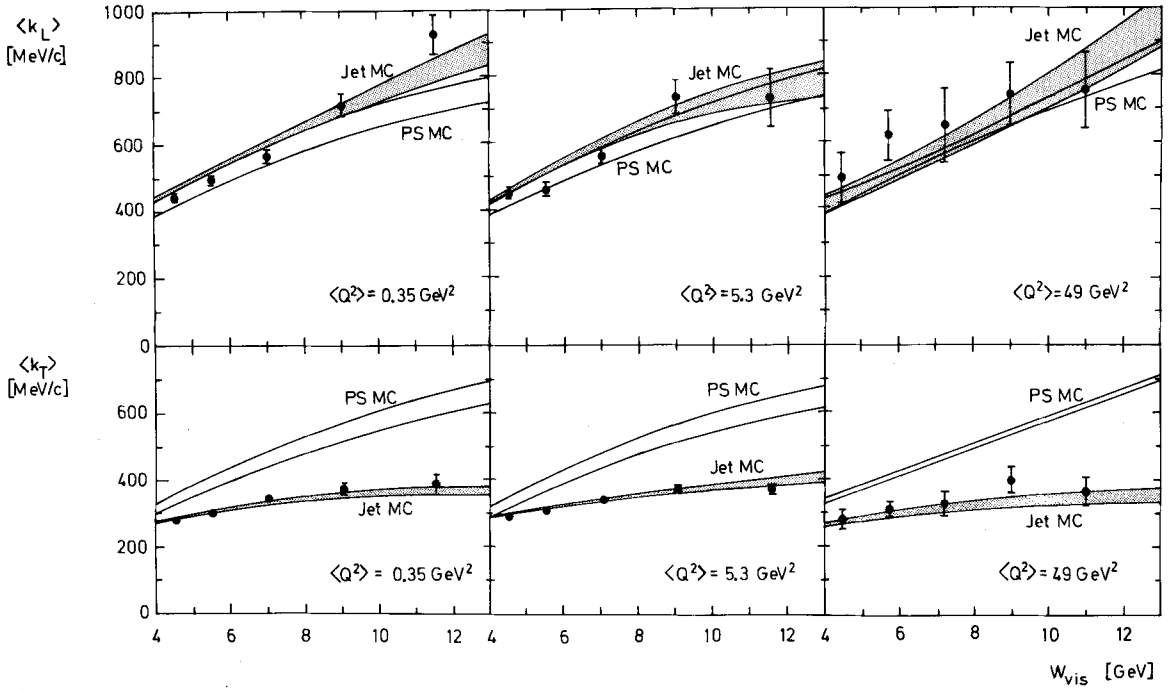

Fig. 3. The average momentum of charged particles transverse and parallel to the reconstructed thrust axis in the hadronic CMS as a function of the visible invariant mass for SAT-, LAT-, and endcap tagged events. The Jet MC band is the expectation from the QPM +VDM described in the text. The PS MC band is the expectation from an all-pion isotropic phase-space hadronization model. The width is due to the range of multiplicities assumed

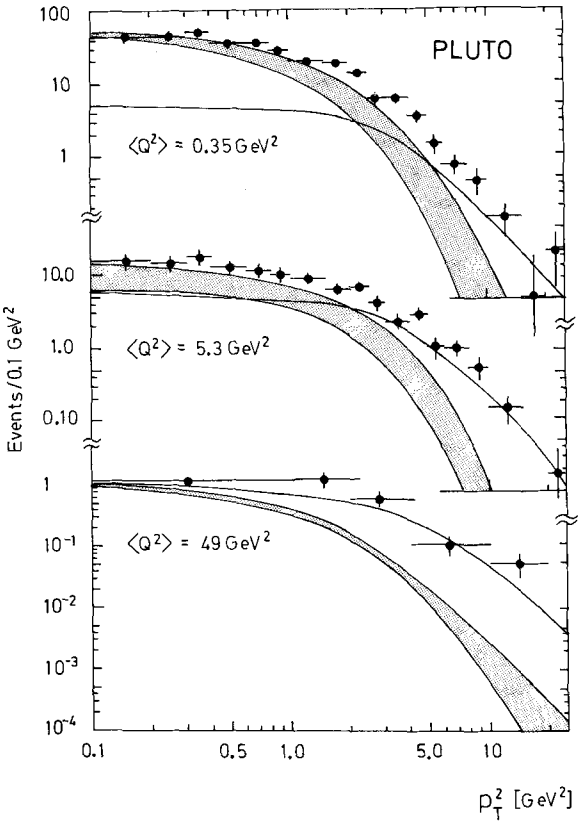

Fig. 4. The observed jet p_T^2 distribution, where p_T is measured with respect to the reconstructed $\gamma\gamma$-axis in the observed hadronic CMS. The solid line is the absolute prediction of the QPM, the band represents the VDM expectation

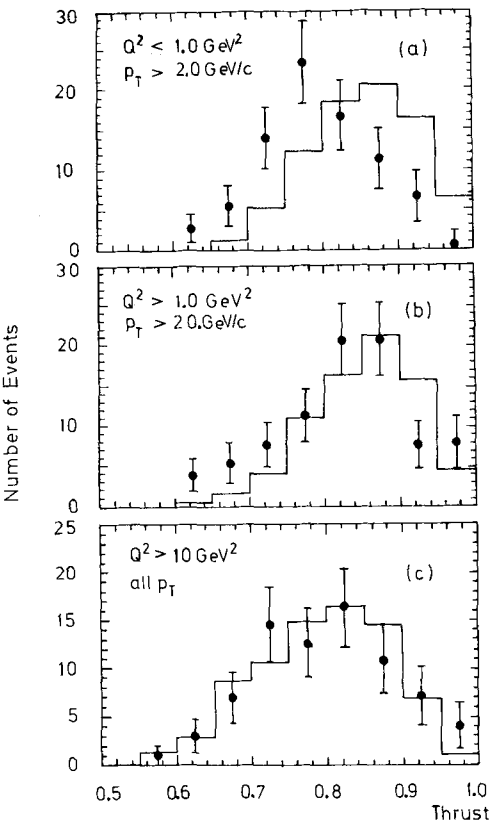

Fig. 5a–c. Observed thrust distributions: **a** and **b** show the low and high Q^2 data for $p_T > 2$ GeV/c. The line is the QPM prediction normalized to the number of events in the plot. **c** Data with $Q^2 > 10$ GeV^2. The solid line is the abolute prediction of QPM

of analysis do not produce a jet-like structure when none is present. These conclusions are not changed if, in the phase space model, 50% of all primary particles are produced as ρ mesons.

Having demonstrated the existence of a two-jet topology, we now examine the jet p_T distributions. They are shown in Fig. 4 for three Q^2 intervals together with the predictions of QPM and VDM. It is evident that for all Q^2 there is an excess of events at high p_T over that predicted by VDM. We take this as evidence for a point-like component in the $\gamma\gamma$ production of hadrons. In addition, for all Q^2, the high p_T events approach the cross section predicted by QPM again indicating the presence of a point-like component.

A point-like component to the $\gamma\gamma$ interaction is expected to result in two-jet events at high p_T; consequently we examine the thrust distribution of the events at high p_T to determine their structure. In Fig. 5a and b we plot the observed thrust distributions for $Q^2 < 1$ GeV^2 and $Q^2 > 1$ GeV^2 for $p_T > 2$ GeV/c. For comparison we show the QPM predictions normalized to the total number of events. It is evident that the low Q^2 events have a lower mean thrust than expected for $q\bar{q}$ events, whereas for $Q^2 > 1$ GeV^2 the data approach the QPM prediction. Since the VDM contribution is expected to be small at all p_T for high Q^2, we show in Fig. 5c the thrust distribution for events with $Q^2 > 10$ GeV^2 summed over all p_T. This distribution agrees both in shape and normalisation with the QPM prediction. We conclude from Fig. 5 that, for $Q^2 > 1$ GeV^2 and $p_T > 2$ GeV/c, or for $Q^2 > 10$ GeV^2 and all p_T, the data have the structure characteristic of $\gamma\gamma \to q\bar{q}$ with the quarks fragmenting as in e^+e^- annihilation.

We now compare in more detail the Q^2 and p_T dependence of the data with QPM. To do this we define the quantity

$$\tilde{R} = \frac{\text{observed number of events at a measured } p_T}{\text{number of events predicted by QPM at that } p_T}$$

If QPM accounted for all observed events, $\tilde{R}_{\gamma\gamma}$ would be equal to unity for all values of p_T and Q^2. In general however, other processes, such as hadronic $\gamma\gamma$ interactions, will make $\tilde{R}_{\gamma\gamma} > 1$. In Fig. 6 we

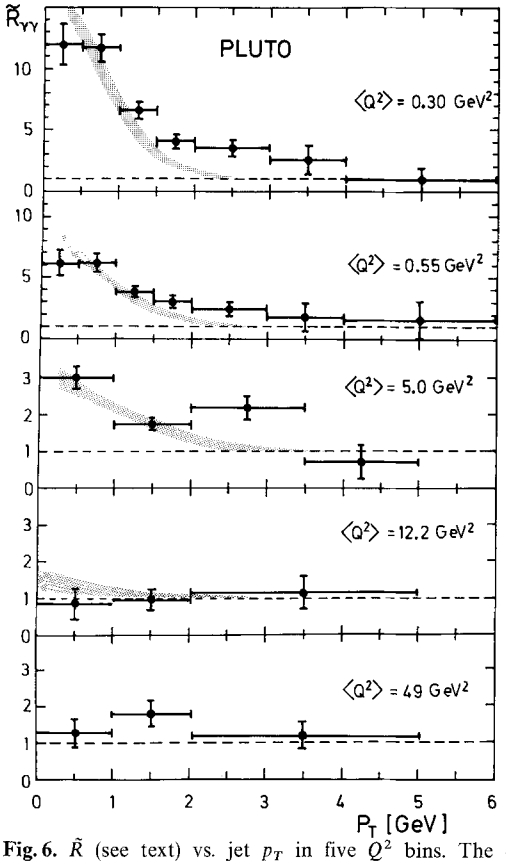

Fig. 6. $\tilde{R}$ (see text) vs. jet p_T in five Q^2 bins. The dashed line shows the QPM expectation (identically one, by definition). The bands give the QPM + VDM prediction; for $\langle Q^2 \rangle$ of 49 GeV^2 the VDM contribution is negligible

show $\tilde{R}_{\gamma\gamma}$ versus jet p_T in five Q^2 bins. The expectations from QPM alone and QPM + VDM are also shown.

From Fig. 6 we observe that

1. For all Q^2 and p_T the data approach the QPM expectation from above as p_T, or Q^2, increases.

2. The Q^2 dependence of $\tilde{R}$ is greatest at low p_T.

3. The p_T dependence of $\tilde{R}$ is greatest at low Q^2.

4. For $Q^2 < 0.4$ GeV^2 and intermediate p_T (2–4 GeV/c) there is an excess of events over the prediction of QPM which is not explained by the VDM used here; this excess may be due to the events that do not have a two-jet structure. In general however, the p_T and Q^2 dependence of the data is well described by the sum of VDM and QPM.

Observations 1 to 3 can be understood in terms of the decrease in the cross section of the hadronic part of the photon relative to the point-like part as Q^2 increases, together with the restriction of the hadronic interaction to the production of mainly low p_T jets. Regarding conclusion 4, we note that QPM + VDM provides a good description of the data. This simple picture of the photon structure as an incoherent sum of a soft, hadronic piece and a hard, point-like component has recently been criticized on theoretical grounds [17]. It is nevertheless interesting that such a picture can describe both the cross section and event topology over a large kinematic region.

Finally we remark that the non two-jet-like events observed at low Q^2 could originate from unresolved multijet events which are predicted to be produced by hadronic and QCD processes in $\gamma\gamma$ interactions. These events could also originate from a direct photon gluon coupling which is predicted in the gauge theory of integrally charged quarks [7, 8]. This would lead to more isotropic events due to the softer fragmentation of gluons [18].

Conclusions

We have demonstrated the existence of jets in the reaction $\gamma\gamma \to$ hadrons in the Q^2 range $0.1 < Q^2 < 120$ GeV^2. The events at intermediate transverse momentum and Q^2 less than 1 GeV^2 look less jet-like than expected from hadron production in $\gamma\gamma$ interactions with standard Field-Feynman fragmentation. At all Q^2 the data show a high p_T tail characteristic of a point-like interaction. The cross section for the production of jets approaches that predicted by the quark parton model for increasing Q^2 or for large jet transverse momenta. These observations are well described in both cross section and event topology by the sum of a hadronic component (described by GVDM) and a point-like component (represented by QPM).

Acknowledgements. We thank the members of the DESY directorate for the hospitality extended to the university groups. We are indebted to the PETRA machine group and the DESY computer center for their excellent performance during the experiment. We gratefully acknowledge the efforts of all engineers and technicians who have participated in the construction and maintenance of the apparatus.

References

1. C. Peterson, T.F. Walsh, P.M. Zerwas: Nucl. Phys. **B174**, 424 (1980); SLAC-PUB-2985 (1982)
2. S.M. Berman, J.D. Bjorken, J.B. Kogut: Phys. Rev. **D4**, 3388 (1971)
3. S.J. Brodsky et al.: Phys. Rev. Lett. **41**, 672 (1978); Phys. Rev. **D19**, 1418 (1979);
K. Kajantie, R. Raitio: Nucl. Phys, **B159**, 528 (1979)
K. Kajantie: Acta Phys. Austriaca, Suppl. **XXI**, 663 (1979);
F A. Berends, Z. Kunszt, R. Gastmans: Nucl. Phys. **B182**, 397 (1981);
W.J. Stirling: Proceedings of the Fifth International Workshop on Photon-Photon Collisions, Aachen, 1983. In: Lec-

ture Notes in Physics. Berger, Ch. (ed.), Vol. 191, p. 142. Berlin, Heidelberg, New York: Springer 1984
4. JADE Collaboration, W, Bartel et al.: Phys. Lett. **107 B**, 163 (1981);
TASSO Collaboration, R. Brandelik et al.: Phys. Lett. **107 B**, 290 (1981);
For a recent review of jet production in $\gamma\gamma$ interactions, see N. Wermes: Aachen proceedings, p. 119.
5. TASSO Collaboration, M. Althoff et al.: Phys. Lett. **138 B**, 219 (1984)
6. For a more detailed presentation of this analysis, see S.L. Cartwright: Ph.D. thesis, University of Glasgow (1983);
A.J. Tylka: Ph.D. thesis, University of Maryland, in preparation.
7. J.C. Pati, A. Salam: Phys. Rev. **D 8**, 1240 (1973); Phys. Rev. **D 10**, 275 (1974); Phys. Rev. Lett. **36**, 11 (1976);
G. Rajasekaran, P. Roy: Phys. Rev. Lett. **36**, 355 (1976);
A. Janah, M. Özer: University of Maryland Technical Report 81–221 (1981);
A. Janah: Ph.D. thesis, University of Maryland (1981);
T. Jayarman, G. Rajasekaran, S.D. Rindani: Phys. Lett. **119 B**, 215 (1982)
8. R.M. Godbole et al.: Phys. Lett. **142 B**, 91 (1984)
9. L. Criegee, G. Knies: Phys. Rep. **83**, 153 (1982);
PLUTO Proposal, Internal Report DESY-PLUTO-79/01 (PRC 79/06) (1979) and Appendix (February 1980);
R.G. Kellogg et al.: Internal Report DESY-PLUTO-84-04 (1984); PLUTO Collaboration, Ch. Berger et al.: Z. Phys. C – Particles and Fields **26**, 199 (1984)
10. PLUTO Collaboration, Ch. Berger et al.: Measurement and QCD Analysis of the Photon Structure Function (in Preparation)
11. J.A.M. Vermaseren: Proceedings of the International Workshop on $\gamma\gamma$ Collisions, Amiens, 1980. In: Lecture Notes in Physics. Cochard, G., Kessler, P. (eds.), Vol. 134, p. 35. Berlin, Heidelberg, New York: Springer 1980;
S. Kawabata: Parallel session talk at the Fourth International Colloquium on Photon-Photon Interactions, Paris, 1981, Proceedings ed. G.W. London, World Scientific Publishing, 1981.
We have also used the event generator described in F.A. Berends, P.H. Daverveldt, R. Kleiss: Instituut-Lorentz (Leiden, The Netherlands) Preprint, August 1983
12. R.D. Field, R.P. Feynman: Nucl. Phys. **B 136**, 1 (1978)
The program we have used for the FF fragmentation is given in T. Sjöstrand, University of Lund Report TP 80-3, April 1980
13. D. Schlatter: SLAC Report No. SLAC-PUB-2982 (1982)
14. G. Hanson et al.: Phys. Rev. Lett. **35**, 1609 (1975);
PLUTO Collaboration, Ch. Berger et al.: Phys. Lett. **78 B**, 176 (1978);
J.L. Siegrist et al.: Phys. Rev. **D 26**, 969 (1982); Phys. Rev. **D 26**, 991 (1982)
15. J.J. Sakurai, D. Schildknecht: Phys. Lett. **40 B**, 121 (1972)
16. I.F. Ginzberg, V.G. Serbo: Phys. Lett. **109 B**, 231 (1982)
17. M. Glück, K. Grassi, E. Reya: University of Dortmund preprint DO-TH 83/23 (1983)
18. JADE Collaboration, W. Bartel et al.: Phys. Lett. **123 B**, 460 (1983)